

# Monitoring Drying, Curing, and ACID-CATALYZED WOOD C

By Ronald T. Obie and  
Cameron Anderson,  
Wood Coatings Research  
Group, Inc.

**F**ast-curing acid-catalyzed alkyd-aminoplast coatings are often utilized as protective coatings for wood cabinet coatings. Quantitative assessment of impact of resin, crosslinker, and catalyst concentration on the curing process can be challenging for these and other coatings as well.

In the development of these coatings, curing is often assessed after the coating film has been exposed to a given cure profile by evaluation of physical properties such as hardness development as a function of time after exiting an oven. Curing under ambient conditions is often assessed by

evaluating coating hardness development as a function of ambient drying-time conditions.

Evaluation of the influence of solvent on cure and crosslinking is often assessed by means of the finger-touch-down method as the sample is drying. Although these methods are very useful, they do not give quantitative insight into the drying and curing of the coating during the early drying process.

The current work investigates the effect of resin and crosslinker composition, and catalyst concentration, on the kinetics of curing of solvent-based acid catalyzed alkyd-aminoplast wood coatings. Further, the research investigates dynamic mechanical thermal properties of the resulting coatings after exposure to a given cure profile.

by EDOT

## Introduction

Acid-catalyzed alkyd-aminoplast coatings for wood coatings applications are commonly based on alkyd resins crosslinked with urea- and/or melamine-formaldehyde crosslinkers and resins. Economical, “water white,” color stable varnishes typically consist of coconut fatty-acid-modified alkyd resin in combination with urea- and/or melamine-formaldehyde crosslinkers. Curing at low temperatures is



# Thermal Properties of ALKYD-AMINOPLAST OATINGS and ADDTR

possible by the addition of a strong acid catalyst such as para-toluene sulfonic acid (PTSA). Rate of cure, development of physical properties, and long-term durability of these varnishes is dependent upon a variety of factors, such as alkyd resin chemistry, crosslinker composition, solvent selection, and catalyst chemistry and concentration.

Alkyd resins may vary in oil type and

length, hydroxyl number and its reactivity (i.e., primary, secondary, etc.), molecular weight, molecular weight distribution, and degree of branching, as well as other parameters.

Aminoplast crosslinkers may be of the urea-formaldehyde (UF) or melamine-formaldehyde (MF) variety. Urea-formaldehyde (UF) crosslinkers display a high tendency to self-condense,<sup>1</sup> typically react faster and at a lower temperature than MF resins and may undergo

crosslinking reaction with the hydroxyl functionality of the alkyd resin as well. Melamine-formaldehyde resins tend to cure more by a transesterification reaction mechanism, although these resins can undergo self-condensation reactions as well,<sup>2,17</sup> especially under high humidity, high temperature, and acid-catalyzed conditions. Reactivity, cure chemistry, and resultant physical properties produced by both crosslinker types is highly dependent upon the alkylating alcohol utilized to synthesize the crosslinker, the amount of alkylation, crosslinker degree of polymerization, catalyst, as well as crosslinker concentration in the final formulation.



## Assessment of Curing

Most practical studies relating to assessment of curing of alkyd-aminoplast coatings typically involve evaluation of hardness development of the cured film as a function of time, temperature, catalyst level, or some combination of these parameters.

Such tests include indentation hardness tests as described in ASTM D 1474,<sup>3</sup> (e.g., Knoop and Pfund hardness numbers); instrumented indentation testing such as those described in ASTM E2546-15;<sup>4</sup> pendulum damping tests such as those described in ASTM D 4366<sup>5</sup> (e.g., König and Persoz Pendulum Hardness Tests); and scratch hardness test such as those performed with pencil, as in ASTM D3353.<sup>6</sup> All these test methods require the coating to have reached some degree of cure and/or hardness development before hardness may be

assessed, thus losing the ability to assess cure of the film in its sol state.

Utilizing gas chromatography to analyze reaction volatiles in polyester coatings crosslinked with various melamine formaldehyde crosslinkers, Blank<sup>7</sup> states that the loss of alcohol from the film by diffusion and/or evaporation has a significant influence on reaction rate of the coating. It is common practice when formulating alkyd-aminoplast coatings to utilize judicious blends and concentrations of alcohols as solvents to help control coating pot life, the rate of flash off, lay open time, and cure rate of the composition. The compositions studied by Blank were typically cured at temperatures of 100 °C or higher for about 20 minutes. He did not look at the influence of variables on cure at early times nor the impact of solvent composition. Blank

proposed a specific acid catalysis mechanism for highly alkylated melamine formaldehyde resins and a general acid catalysis mechanism for partially alkylated resins and/or fully alkylated, high-imino resins. The reaction schemes proposed by Blank for these two cure mechanisms are shown in Figures 1 and 2, respectively.

From these reaction pathways, it is seen that not only is the formulation solid composition important to determining cure, but solvent selection can display an important influence on the early cure response of the coating system. In this work, we consider cure response of alkyd-aminoplast coatings from application through consolidation under low temperature cure conditions by use of evaporative dynamic oscillation (EDOT)<sup>8</sup> and/or automated dynamic drying time recorder (ADDTR).<sup>9</sup>

**FIGURE 1**

Specific acid-catalysis mechanism proposed by Blank for highly alkylated melamine formaldehyde resins reacting with primary polyols. (Reproduced according to reference 7.)

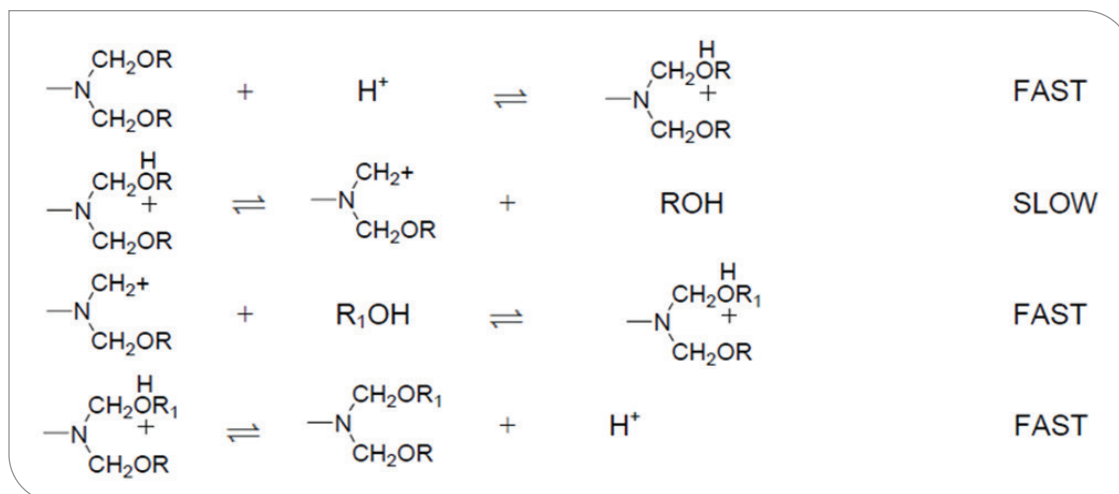
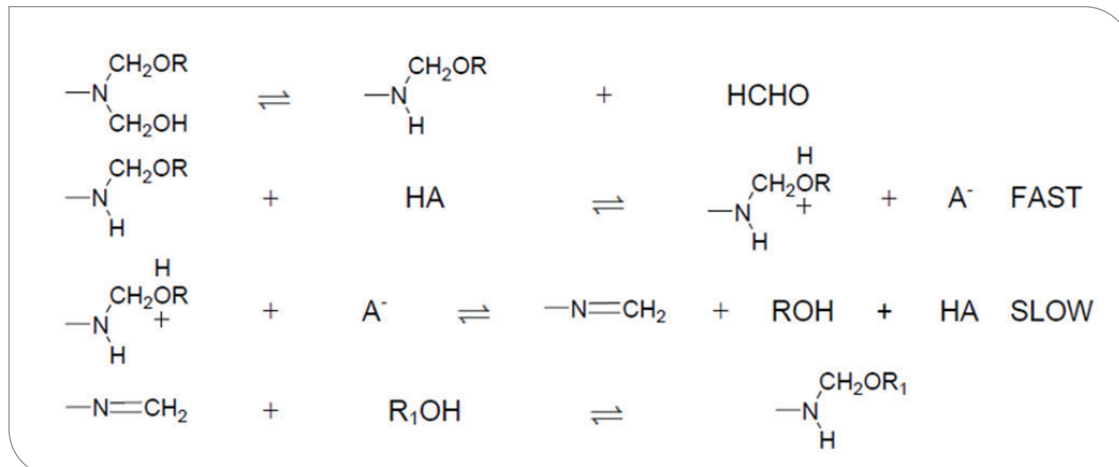


**FIGURE 2**

General acid-catalysis mechanism proposed by Blank for partially alkylated and/or highly alkylated high-imino melamine formaldehyde resins reacting with primary polyols. (Reproduced according to reference 7.)



## Experimental

All resins and polymers, formulations, and formulation constituents, including solvents, were utilized as received from the supplier.

### Evaporative Dynamic Oscillation (EDOT)

The EDOT test has been described previously.<sup>8,10</sup> Evaluation of films for drying and curing was conducted utilizing a 25 mm EDOT probe attached to a MCR 301 research grade rheometer from Anton Paar GmbH, Graz, Austria. The rheometer was equipped with a Peltier hood capable of flooding the hood area with low-humidity air. Before entering the hood area, the air was dried through a series of driers. Relative humidity of the air at 25 °C was found to range between 4 and 12% RH. Briefly, films were cast onto a bottom plate equilibrated to 25 °C, and having a diameter of 60 mm and a well depth of 150 microns.

Typically, the EDOT probe was positioned approximately 100 microns from the bottom of the plate after having been initially dipped to 20 microns. Generally, approximately 1.5 minutes elapsed between application of the coating to bringing the probe to its measurement position. The probe was rotated in the sample for 3 seconds at a shear rate of 25 s<sup>-1</sup>, and then allowed to sit in the sample for an additional 60 seconds at 0 s<sup>-1</sup>. This was followed by a normal force reset. After an additional 10 seconds at 0 s<sup>-1</sup>, the test was initiated while simultaneously flooding the hood with low-humidity air at an airflow rate of 50 L/hr. In total, about 3 minutes elapsed between loading the sample and beginning the cure-profile portion of the test.

The cure profile consisted of ramping the temperature from 25 °C to 35 °C during a 30-second interval. The temperature was held at 35 °C for 270 seconds, and then the temperature was ramped from 35 °C to 65.6 °C for 30 seconds. The temperature was held at 65.6 °C for an additional 270 seconds, before ramping the temperature back down to 25 °C over a period of 60 seconds. The sample was held at 25 °C for 540 seconds before additional testing was conducted. The test was conducted in dynamic oscillation mode during the curing profile utilizing a shear strain of 0.1% and an angular frequency of 10 1/s.

After a total of about 2 hours from application, the temperature of the sample was decreased from 25 °C to -20 °C for 60

minutes, and then held at -20 °C for an additional 60 minutes. A DMTA sweep was then conducted on the sample from -20 °C to 110.4 °C over a period of 67.2 minutes. The sample was held at 110.4 °C for 1 hour before ramping down to 25.4 °C for 43 minutes. The DMTA test was conducted at a shear strain of 0.2% and angular frequency of 10 1/s.

### Automated Dynamic Drying Time

The method for using the Automated Dynamic Drying Time Recorder (ADDTR) to measure drying time and hardness development over time is detailed in references 9 and 11. The testing conducted in this current work generally followed those same procedures. Films to be evaluated were cast onto a clear plate glass with a 3-mil bird bar utilizing a byko-drive automatic drawdown machine available from BYK Gardner USA, noting the actual time of drawdown. The drying times of the films were recorded under atmospheric conditions for approximately 2 hours at a platform-translation testing rate of 0.021 mm/s while maintaining a load of 10 grams.

### Hardness of drying and/or cured films

To test scratch hardness, films were applied with a 6-mil bird bar onto glass substrates. The films were then evaluated for their scratch hardness over time, either from the moment of application or from the time they exited the oven. Unless otherwise noted, films were force dried according to the following schedule: flash 5 minutes, force dry 5 minutes at 35 °C, followed by 5 minutes at 65 °C, and then cool 10 minutes. Film hardness on glass substrate was evaluated by a progressive load normal force technique utilizing a testing probe consisting of a hardened stainless steel loop probe available from BYK Gardner USA attached to a stainless-steel stylus. For the work reported on in this report (see Figures 15 and 16) scratch hardness progressive load tests were conducted over 120 mm at a platform translation rate of 12.7 mm/s at a normal force loading rate of 3.175 N/s from approximately 0 – 30 N. Tests were conducted at least twice, and the average failure load reported for each time stamp evaluation. Failure loads were determined visually, as well as by stereoscopic examination, by determining the distance at which failure occurred, and then matching the

**The current work investigates the effect of resin and cross-linker composition, and catalyst concentration, on the kinetics of curing of solvent-based acid catalyzed alkyd-aminoplast wood coatings.**

measured distance to an exact measured load associated with that distance.

Various failure modes were identified,<sup>11</sup> depending on the test. These modes included load-to-surface mar, surface scratch, stick-slip, stomata crack, and complete failure. The last mode, depending upon the substrate, included significant cracking/delamination of coating and/or removal of coating from the substrate.

Load-to-surface mar is where the surface of the coating begins to be disrupted, resulting in either by a change in gloss or indentation of the surface. Load-to-scratch is where the surface is scratched, usually resulting in a slight cut into the surface of the coating film or a slight whitening of the surface.

Load-to-stick-slip is where there is a visible wave pattern left in the film where the probe has traveled; usually this wave pattern appears as a series of concentric "V"s or "U"s in the film when viewed under grazing angle light through a low-power stereoscope; load to stomata crack is that load where small cracking begins to be seen in the track left by the probe; usually these cracks appear as mouth-shaped circles that appear, at least at the macro scale, as the shape of open stomata cells in tree and plant leaves and stems.<sup>12</sup> In plants, stomata cells are responsible for releasing moisture from the leaves of the plant and absorption of carbon dioxide from the atmosphere during the transpiration process.

Load-to-complete failure, depending upon the substrate, is that load where the coating is either completely removed from the substrate and/or there is a high density of film cracking, and/or stomata cracking has extended from small individual cracks to areas where large amounts of coating is removed from the substrate. In this report, stomata-cracking failure was utilized to quantify hardness.

## Results and Discussion

### Impact of PTSA Acid Catalyst Concentration on Cure Rate of an Acid-catalyzed Varnish

Figures 3 and 4 display EDOT drying profiles of an acid-catalyzed varnish. Figure 3 displays the drying of the sample without catalyst, while Figure 4 is the same sample catalyzed with 5.4 wt % PTSA solution. In both figures, solid square symbols represent storage modulus values; solid triangles represent loss modulus; solid circle symbols represent complex viscosity; solid diamond symbols represent tan delta; and the line without symbols represents temperature.

There are several notable similarities and differences in drying/cure behavior displayed between the uncatalyzed and catalyzed sample. First, both samples display an increase in viscosity and modulus with time and temperature during the first two temperature profile ramps. However, the uncatalyzed sample of Figure 3 displays viscous behavior throughout the force dry schedule. The results indicate limited to no crosslinking, and hence, the change in modulus and viscosity appears to be strictly due to solvent evaporation.

The catalyzed sample of Figure 4 shows a crossover point at about 270 seconds of curing time (7.43 minutes total cure time) (solid

blue symbols) where the sample begins to display a greater solid-like behavior compared to viscous-like behavior. Additionally, the viscosity and modulus curves of the sample with catalyst increase more rapidly and are greater throughout the drying profile. Tan delta values (the ratio of loss to storage) for the catalyzed sample are smaller throughout the curing profile, indicating more complete drying/curing for the catalyzed sample.

Figure 5 displays data and best-fit linear regression of cure time, as measured by storage modulus/loss modulus crossover time, versus the wt % catalyst determined from data that was obtained, which is displayed in Figures 3 and 4. The black line and symbols

**FIGURE 3**

The EDOT drying profile for acid-catalyzed varnish without catalyst. Strain = 0.1%,  $\omega$  = 10 1/s; 25 mm EDOT probe.

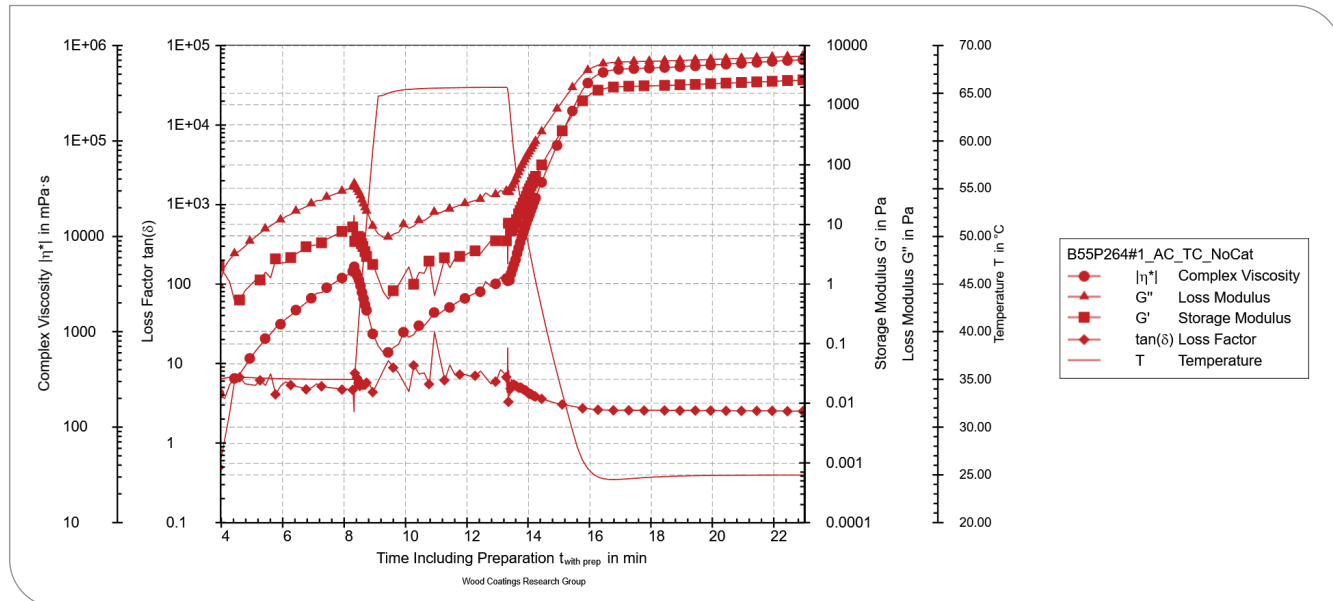


**FIGURE 4**

The EDOT drying profile for acid-catalyzed varnish catalyzed with 5.4 wt % PTSA soln. Strain = 0.1%,  $\omega$  = 10 1/s; 25 mm EDOT probe.

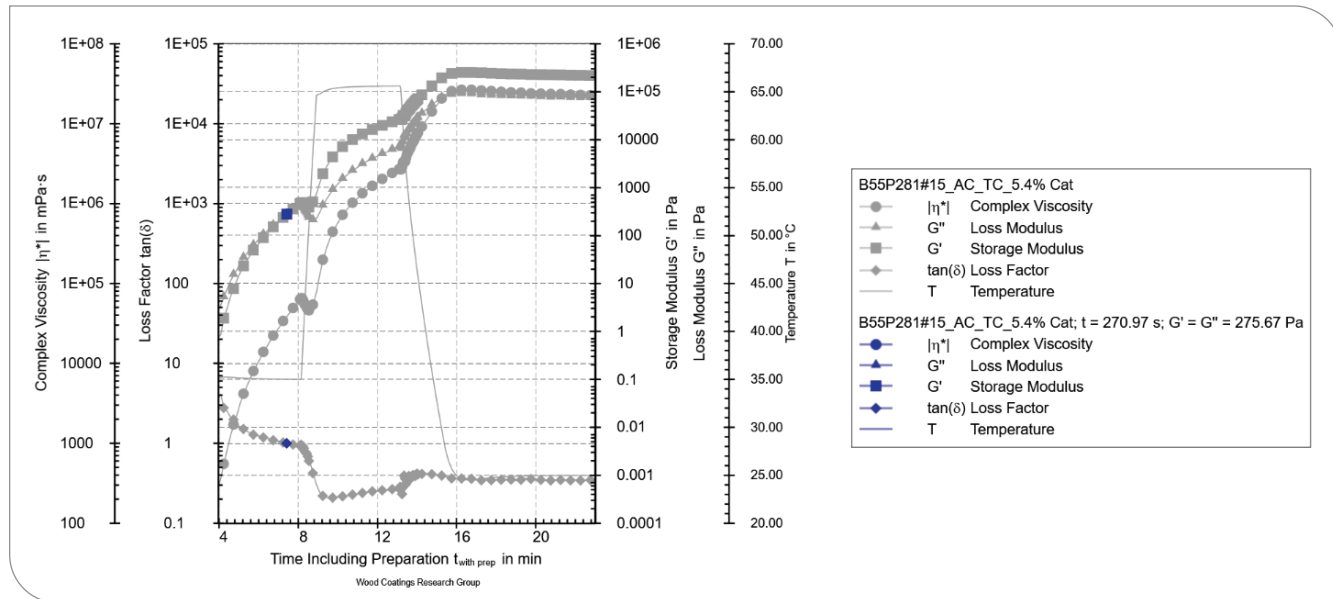


**FIGURE 5**

Storage modulus/loss modulus crossover time vs. wt % catalyst. The black curve and symbols are those where  $t_0$  taken as time of coating application. The green curve and diamond symbols are those where  $t_0$  is taken from start of cure profile.

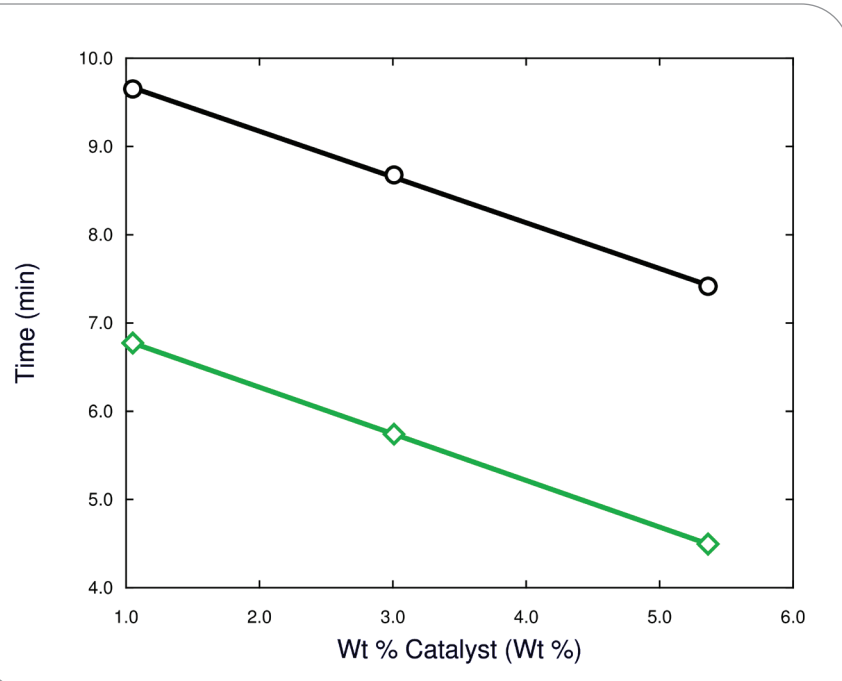
**TABLE 1**  
Regression Constants for Data of Figure 5

Figure 5 Curve	T <sub>0</sub> Time	Slope	r <sup>2</sup>
Black curve and symbols	From time of sample application	-0.52	0.9996
Green curve and symbols	From beginning of cure profile	-0.53	0.9988

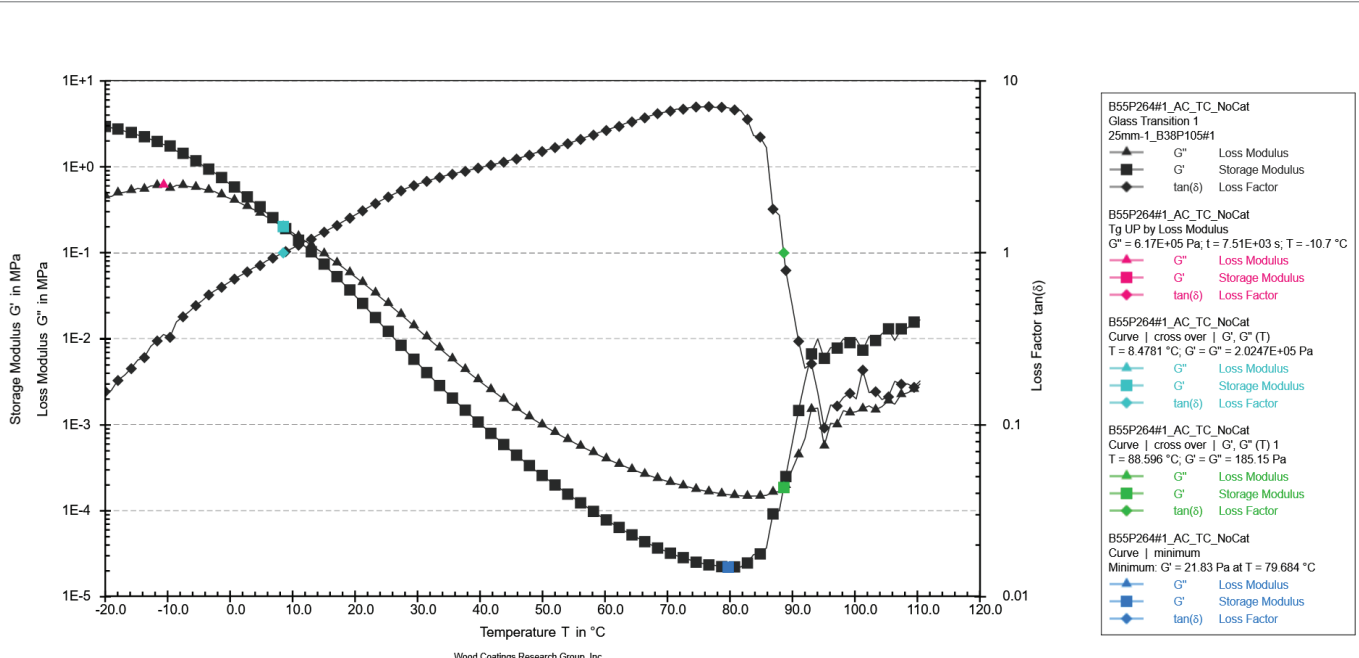
are for results analyzed for time where the zero start time is the time of application of the sample, whereas the green line and symbols are for results analyzed when the cure profile was started. Regression results are given in **Table 1**. As expected, essentially both methods of analyzing the data produce in the same slope value.

The data indicate that for every 1% increase in catalyst, time to reach sol-gel is reduced linearly by just over 30 seconds, within the limits of the 1 wt % to 5.4 wt % catalyst addition. The linear behavior of the cure as determined by sol-gel cure is particularly intriguing since cure for these samples occurred across a range of times within the total cure profile. For instance, sol-gel crossover occurs during the 65 °C portion of the curing profile for 1 wt % catalyst addition, within the 35 °C to 65 °C temperature ramp for the 3 wt % catalyst addition, and in the 35 °C curing profile for the 5.4 wt % catalyst addition.

**Figure 6** is a DMTA curve for the acid-cure varnish film without catalyst after the film has aged about 3 hours from the time of application, inclusive of having been exposed to the cure profile described above and brought to -20 °C and held for 1 hour. Data are shown from -20 °C to 110.4 °C. In the figure, solid square symbols represent storage modulus values; solid triangles represent loss modulus values; solid diamonds represent loss factor values.

**FIGURE 6**

In situ EDOT DMTA curves for acid-catalyzed varnish without catalyst after 3 hours from time of application. Strain = 0.2%;  $\omega = 10$  1/s; 25 mm EDOT probe. See text for symbol designation.



represent tan delta values. The figure displays several interesting characteristics worth noting.

First, the data indicates that the uncured sample displays solid-like behavior at -20 °C, which, based on unpublished results appears primarily due to the  $T_g$  of the short oil coco-nut alkyd.

Second, the loss modulus curve displays a maximum at about -10.7 °C (solid pink triangle); this value is taken as the glass transition value as measured by loss modulus.

Third, there is an initial temperature proceeding from -20 °C at which the loss modulus begins to exceed storage modulus values. This temperature is about -8.5 °C, shown by the solid light blue square and diamond. The fact that the sample displays this type result indicates that the sample without catalyst is uncured and displays thermoplastic like behavior. However, as the temperature is increased, there is a temperature at which the storage modulus displays a minimum and thereafter begins to increase. This temperature is found to be 79.7 °C and is indicated by the solid dark blue square in the storage modulus curve. This data point indicates a cure-activation temperature for the sample but may also include some further loss of residual solvent from the film.

Lastly, the solid green square and diamond symbols represent the temperature at which the storage modulus value begins

to dominate over the previously greater loss modulus values. This temperature is found to be approximately 88.6 °C in this experiment and represents the temperature at which the uncatalyzed sample cures.

**Figure 7** compares the DMTA curves for the acid-cure varnish with 1 wt % catalyst to those for the sample without catalyst as displayed in **Figure 6**. For clarity, the previously discussed “noted” data points of interest have been removed from the sample with 0% acid catalyst and added to the red curves of the 1% catalyzed sample. Further, the 1 wt % catalyzed sample DMTA data are obtained after about 3.4 hours from time of application.

As shown in **Figure 7**, the DMTA curves of the sample with catalyst is significantly different than that without catalyst. First,  $T_g$  as measured by the initial maximum in the loss modulus curve and displayed by the solid green triangle symbol occurs at about 6.8 °C, 17.5 °C greater than the uncatalyzed sample.

Secondly, there is no crossover between storage modulus and loss modulus curves, indicating that at the time of analysis, the 1 wt % catalyzed sample displays thermoset or crosslinking behavior.

Thirdly, the solid blue square symbol on the storage modulus curve at about 48.9 °C indicates the temperature where cure is further activated for the 1 wt % catalyzed sample. The cure-activation temperature for the 1 wt % catalyzed sample is significantly

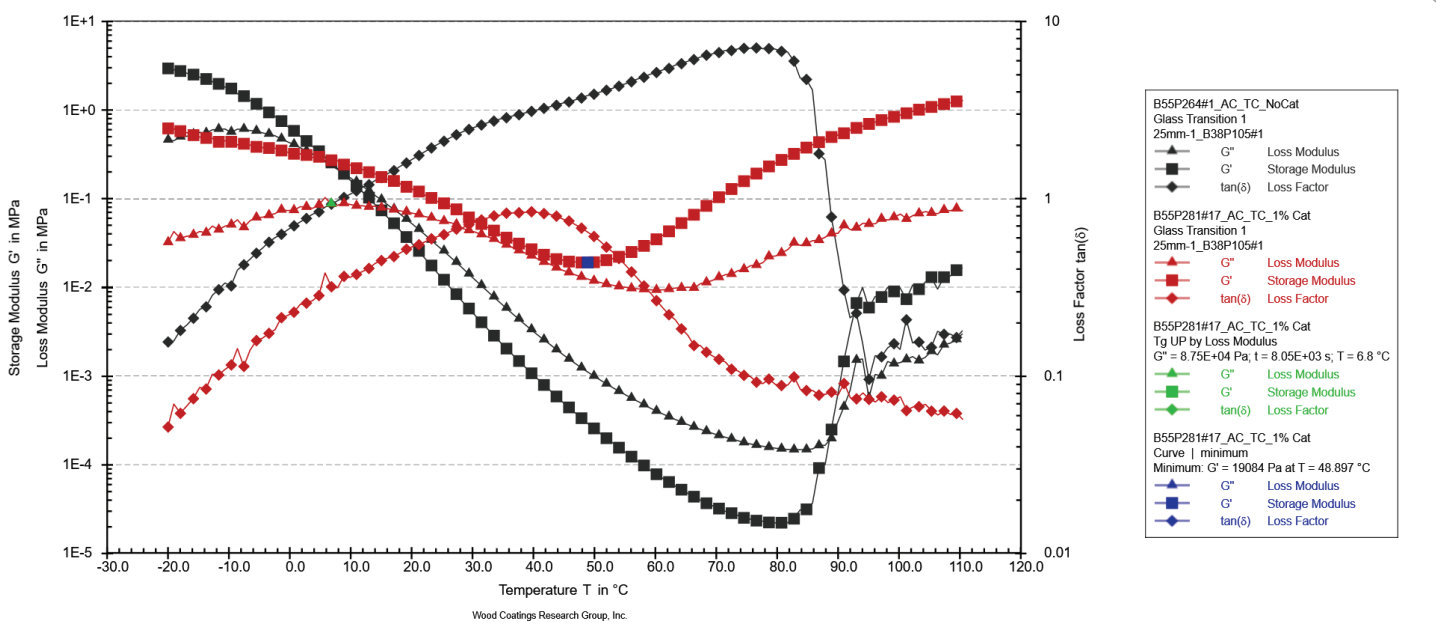
lower than sample without catalyst. This data point is further significant as it indicates that if a sample in the field having these cure characteristics were to be exposed to a temperature in excess of about 48.9 °C, one might expect additional crosslinking to occur, and hence, the possibility of sample embrittlement and potential failure.

**Figure 8** displays data and best-fit curve for  $T_g$  (K) as determined by maximum in loss modulus curve, versus % wt catalyst, for the acid-cure varnish. The data were fit to a monomolecular model by the freely available program Simfit.<sup>13</sup> The representative model and calculated parameters for the curve of **Figure 8** are given in **Table 2**. The data of **Figure 8** indicate that there is not much to be gained from a  $T_g$  standpoint by increasing the catalyst concentration beyond about 5.4 wt %.

**Figure 9** displays data and best-fit curve for post-cure-activation temperature ( °C) as a function of wt % catalyst. The data are fit to a Von Bertalanffy 2/3 model with Simfit.<sup>13</sup> The representative model and calculated parameters for the curve of **Figure 9** are given in **Table 3**. The data of **Figure 9** indicate that post-cure-activation temperature is dramatically lowered by the addition of a small amount of catalyst and does not change significantly with further catalyst addition.

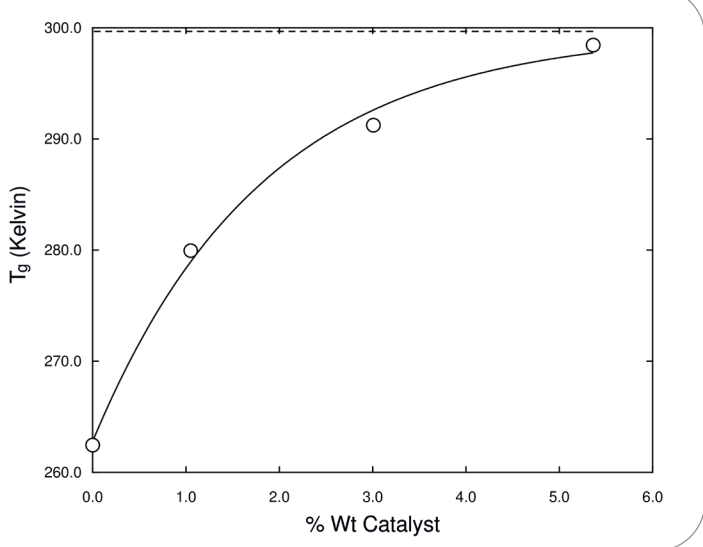
**Figure 10** is a DMTA plot displaying storage modulus curves as a function of

**FIGURE 7**  
In situ EDOT DMTA curves for acid-catalyzed varnish with 1 wt % catalyst, represented by red curves and symbols, vs. without the catalyst, represented by black curves and symbols, after 3.4 and 3 hours, respectively, from time of application.  
Strain = 0.2%,  $\omega$  = 10 1/s; 25 mm EDOT Probe.

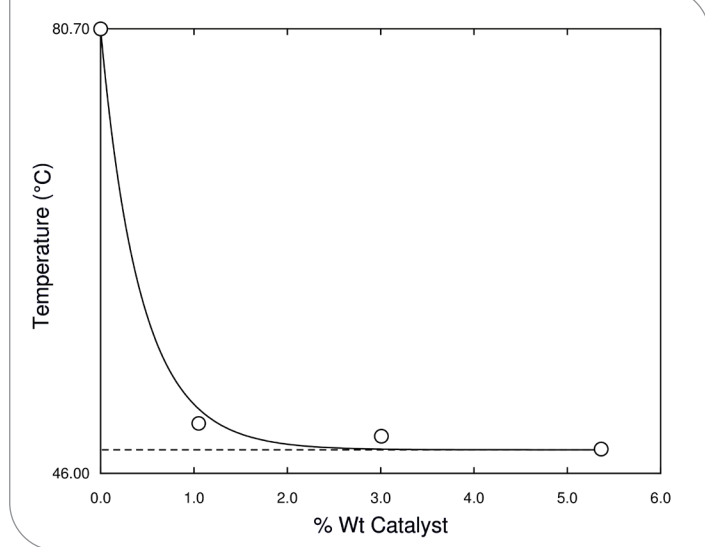


**FIGURE 8**

The effect of wt % catalyst on loss modulus based glass-transition temperature for acid-catalyzed varnish.

**FIGURE 9**

The effect of wt % catalyst on post-cure-activation temperature for acid-catalyzed varnish.

**TABLE 2**

Calculated Parameters for Representative Model of Figure 8

Failure Criteria Evaluated	Model Fitted	R <sup>2</sup>	Parameter	Parameter Value	Calculated Parameter Standard Error	Max. Observed Growth Rate
T <sub>g</sub> by Max. in Loss Modulus Curve	S(t)=A(1 - Be <sup>(-kt)</sup> ); B = 1-(S <sub>0</sub> /A)	0.9953	A	299.69	2.8371	20.260
			B	0.12315	0.00922	
			k	0.54897	0.12462	

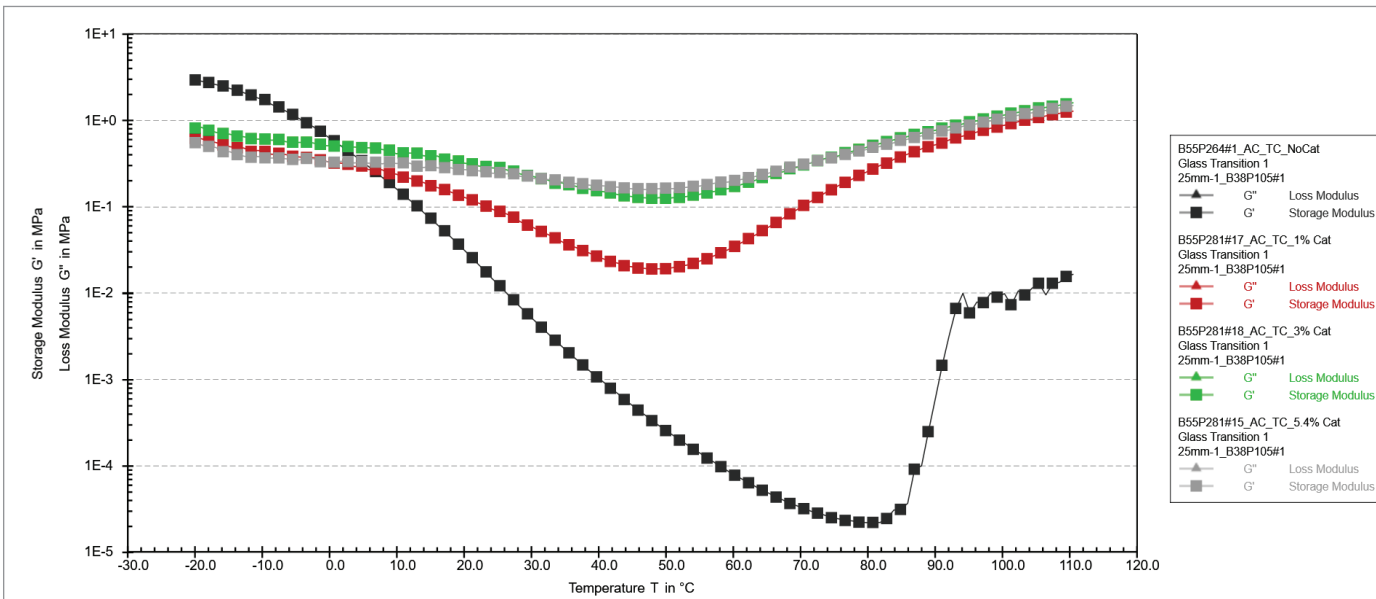
**TABLE 3**

Calculated Parameters for Representative Model of Figure 9

Failure Criteria Evaluated	Model Fitted	R <sup>2</sup>	Parameter	Parameter Value	Calculated Parameter Standard Error	Minimum Observed Growth Rate
Cure Activation Temperature after T <sub>g</sub>	S(t)=[A <sup>1/3</sup> - Be <sup>(-kt)</sup> ] <sup>3</sup> ; A <sup>1/3</sup> = η/κ; B = η/κ - S <sub>0</sub> <sup>1/3</sup> ; k = κ/3	0.9970	eta	-22.472	6.0009	-79.766
			kappa	-6.1904	1.6254	
			S <sub>0</sub>	47.837	1.0986	

**FIGURE 10**

Effect of wt % catalyst on storage modulus during DMTA test for acid-catalyzed varnish. 0% catalyst is represented by black symbols; 1% catalyst is represented by red symbols; 3% catalyst is represented by green symbols; 5.4% catalyst is represented by gray symbols.



temperature and wt % catalyst. The data show that as the catalyst level increases, the minimum modulus displayed by the sample in the temperature ramp increases. Further, there is less change in modulus as the temperature is increased further beyond that where the minimum takes place. The data indicate that increasing the catalyst concentration increases crosslinking density as well. However, there is less change in modulus as temperature is increased beyond the minimum as catalyst concentration is increased. This suggests that cure should be optimized for catalyst and temperature to maintain a minimum change in film

properties should the sample be exposed to temperatures above the cure-activation temperature while in service.

Another method of cure assessment involves evaluating the increase in storage modulus, loss modulus, and/or complex viscosity as a function of time and catalyst concentration, and then fitting the data to obtain kinetic parameters. **Figures 11** and **12** display the influence of acid-catalyst concentration on complex viscosity growth at the 35 °C and 65 °C stage of cure, respectively. The figures indicate that rate of cure as measured by viscosity growth increases with catalyst concentration and

cure temperature. At 35 °C, solvent evaporation appears to play an important role in viscosity increase. The data also indicate that at 65 °C, similar cure is obtained by 3 wt % and 5.4 wt % catalyst addition.

Log complex viscosity was modeled utilizing a  $T_1$ -form Unified Richard's growth model (shown in equation (1)) as described by Tjørve.<sup>14,15</sup> The  $T_1$ -form of the equation yields the inflection time parameter. Further, the unified model allows comparison of parameters to other unified models such as the Unified Gompertz.<sup>14</sup> The model shown yields the relative growth rate (e.g., relative to the asymptote, A).

**FIGURE 11**

The effect of wt % catalyst on viscosity at 35 °C for acid-catalyzed varnish. 0% catalyst is represented by black symbols; 1% catalyst is represented by red symbols; 3% catalyst is represented by gray symbols; 5.4% catalyst is represented by blue symbols.

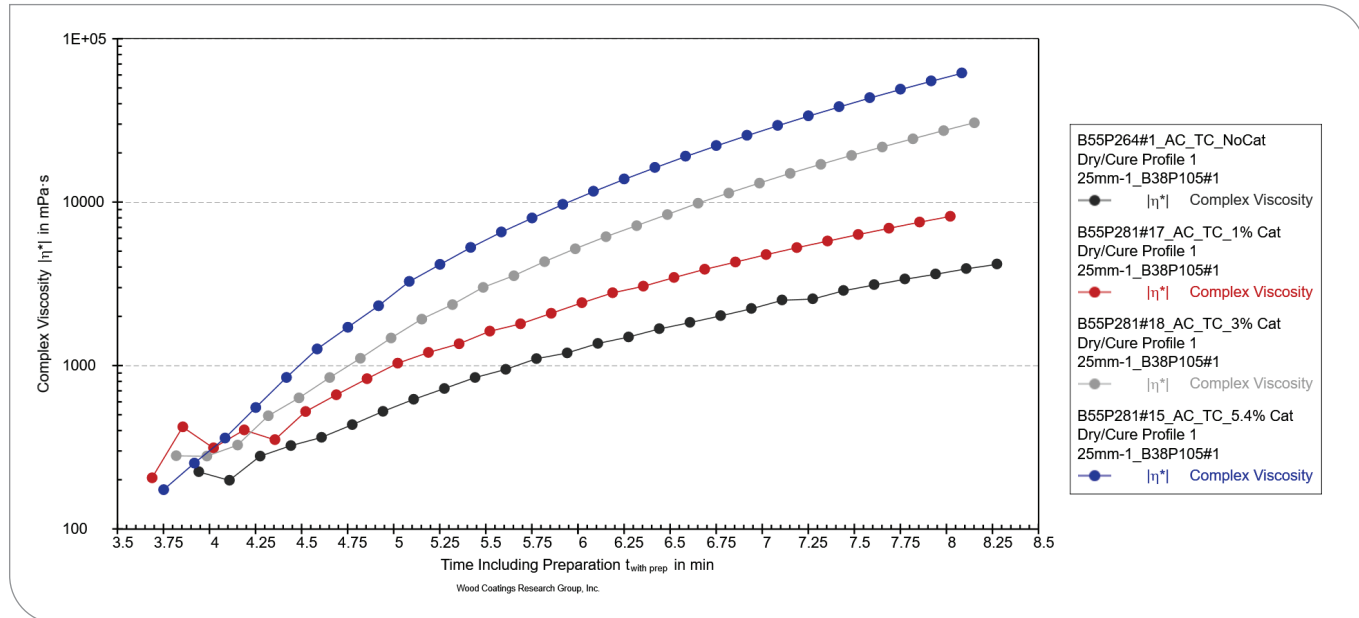
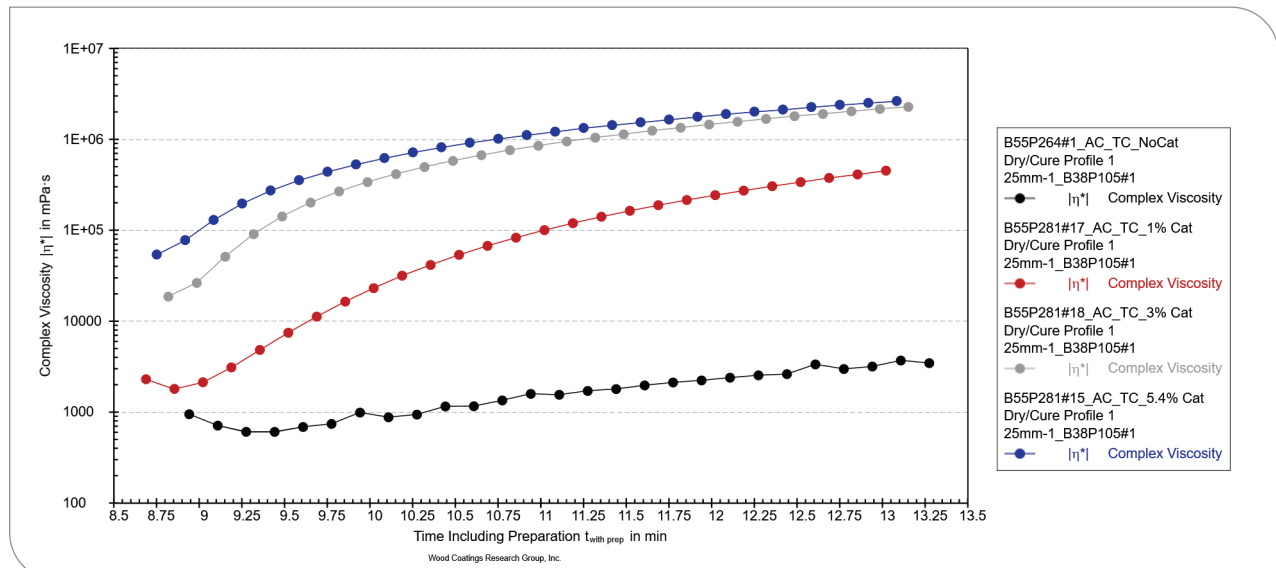


**FIGURE 12**

The effect of wt % catalyst on viscosity at 65 °C for acid-catalyzed varnish. Black symbols are 0% catalyst; red symbols are 1% catalyst; gray symbols are 3% catalyst; and blue symbols are 5.4% catalyst.



$$W(t) = A \left[ 1 + (d-1) \cdot \exp \left[ \frac{-k_u(t - T_i)}{d^{(d-1)}} \right] \right]^{(1/(d-1))} \quad \text{EQ 1}$$

Where:

- $W(t)$  is the measured value at time  $t$ , in our case log complex viscosity
- $A$  is the upper asymptote
- $k_u$  maximum relative growth-rate constant as found at inflection
- $T_i$  time at inflection
- $d$  parameter shifting the inflection value

**Figure 13** gives examples of modeling 3 wt % catalyst added to the acid-cure-varnish cured at 35 °C and 65 °C utilizing **Equation 1**. **Table 4** summarizes the calculated model parameters found for films cured through the 35 °C and 65 °C cure protocols.

**Figure 14** displays regression curves (data and best-fit line) for the Unified Richards model determined relative rate constant, versus catalyst concentration for the two cure temperature protocols. The program SimFit<sup>13</sup> was utilized to fit the data.

The data for 35 °C show that the rate constant increases as catalyst concentration is increased, displaying a maximum rate at the maximum catalyst concentration; the data are best described by a Von Bertalanffy 2/3 model  $\{S(t) = [A^{1/3} - B \exp(-kt)]^3\}$ ; where  $A^{1/3} = \eta/\kappa$ ,  $B = \eta/\kappa - S_0^{1/3}$ ,  $k = \kappa/3$ .

On the other hand, the data for 65 °C show that the rate constant levels off at about 5.4% catalyst; the maximum rate constant increase occurs at about 1.05% catalyst. The data are best described by a logistic model  $\{S(t) = A/[1 + B \exp(-kt)]\}$ ; where  $B = A/S_0 - 1$ .

**TABLE 4**  
Calculated Parameters Determined for Unified Richards Model (EQ 1)  
for Drying/Curing of Acid-Catalyzed Varnish at 35 °C and 65 °C

% Catalyst	Cure Temp., C	A (P1)	K <sub>u</sub> (P2)	T <sub>i</sub> (P3)	d (P4)	r <sup>2</sup>
0	35	4.16838	2.87922E-01	1.26656	-6.59488E-07	0.9990
1.05	35	4.56738	2.89994E-01	1.35831	2.07252E-05	0.9992
3.008	35	5.25631	3.09684E-01	2.01955	-2.87538E-07	0.9996
5.3634	35	5.34626	3.87196E-01	2.36598	-3.43125E-07	0.9994
0	65	4.25090	1.26605E-01	4.40772	2.57899E-01	0.9863
1.05	65	5.97517	3.21837E-01	7.65820	2.88969E-01	0.9996
3.008	65	6.41586	6.51577E-01	6.87676	-1.00000E+00	0.9969
5.3634	65	6.45581	6.95945E-01	6.82829	-1.04726E-05	0.9958

**FIGURE 13**  
Data and best-fit lines for acid-catalyzed varnish catalyzed with 3 wt % catalyst; unified Richards fit (EQ 1) of log complex viscosity. Circle symbols represent the 35 °C cure profile; square symbols represent the 65 °C cure profile.

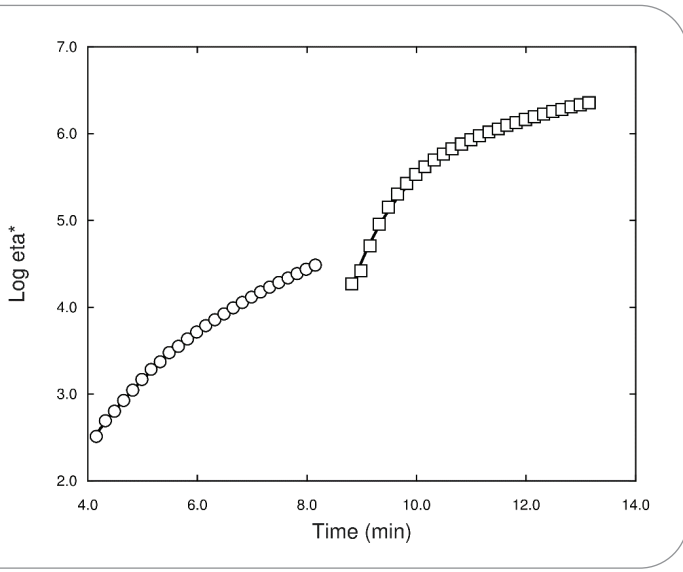


**FIGURE 14**  
Data and best-fit lines for maximum relative growth rate constant as a function of catalyst concentration for 35 °C and 65 °C cure profiles. The black curve and open circle symbols are for 35 °C cure profile, r<sup>2</sup> = 0.9997; the aqua dashed line and square symbols are for 65 °C cure profile, r<sup>2</sup> = 0.9998.

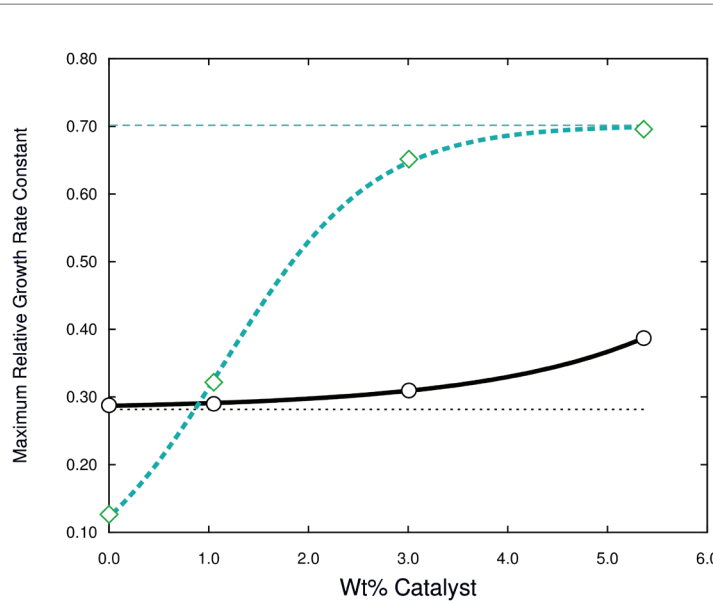


**Figure 15** displays the scratch hardness of a 6-mil bird bar drawdown application of the acid-cure varnish catalyzed with 5.4 wt % PTSA solution, as a function of time. The data represented by open circles are load-to-stomata cracking. The data were

obtained by use of an ADDTR reconfigured to measure scratch hardness by a progressive loading method as discussed in reference 11.

The solid square data point represents the scratch hardness of the sample 5

minutes after application of the sample where the sample is still in its sol state. The open circles represent the scratch hardness of the sample from time of exiting the final 65 °C cure oven (e.g., the first data point is obtained approximately 10 minutes after exiting the final cure oven). The solid black line is a best-fit line utilizing a monomolecular model of the open circle data ( $r^2 = 0.9710$ ).

As shown in **Figure 13**, it is clear from the data of **Figure 15** that the sample cures rapidly when exposed to the cure profile (5 minutes at 35 °C, 5 minutes at 65 °C). It is also intriguing to consider that the scratch hardness as measured in the 2-hour to 3-hour range may be able to be correlated with the measured glass-transition temperature as displayed in **Figure 8**.

**Figure 16** compares cure of the neat topcoat sample as shown in **Figure 15** (open black circle and best-fit line (solid black)) to the cure of the same topcoat in a full coating system, e.g., 2 coats of solid stain, 1 coat of sealer, followed by 1 coat of topcoat applied by 6 mil bird bar (represented by open black square symbols). The dashed black line is a best logistic fit to the open black symbol data ( $r^2 = 0.9990$ ).

The data show that the undercoat system has a noticeable effect on the scratch hardness of the topcoated and finished system, lowering the scratch resistance as determined by cracking.

**Figure 17** compares the effect of urea-formaldehyde (UF) crosslinker on drying results of an acid-catalyzed varnish. Each formulation consisted of the same PHR UF resin, melamine formaldehyde crosslinker modifier, and short oil coconut alkyd. Each formulation was catalyzed with the same amount of PTSA catalyst (4.97% (w/w)).

All three UF resins are described as “partially isobutylated” resins. UF1 and UF3 have similar urea/formaldehyde/isobutanol ratios, but UF3 is stated to be higher in molecular weight. UF1 and UF2 are stated to be partially soluble in aliphatic and aromatic hydrocarbons, whereas UF3 is partially soluble in aliphatic hydrocarbons but soluble in aromatic hydrocarbons.

Solvent composition for the formulations is similar although a slight adjustment was required for UF3 due to the solvent system for which it is supplied (e.g., 5.2 wt % n-butanol replaced as isobutanol and 0.6 wt % ethanol replaced as isobutanol).

**FIGURE 15**

Data and best-fit lines for scratch-hardness development as a function of time out of the force-dry-cure oven for acid-cure varnish catalyzed with 5.4% (w/w) acid catalyst (represented by the open circles and solid black line). The solid black square is data for the sample 5 minutes after application. Scratch hardness was obtained as load-to-stomata cracking for the open circle data.

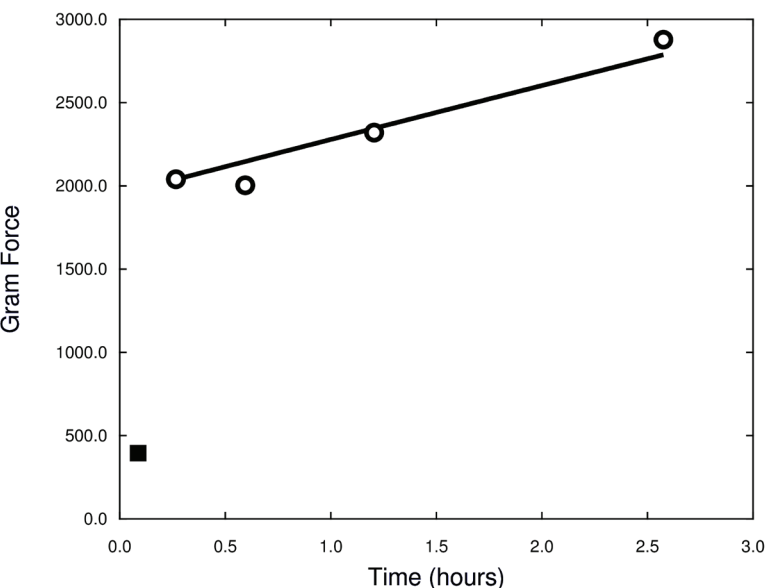
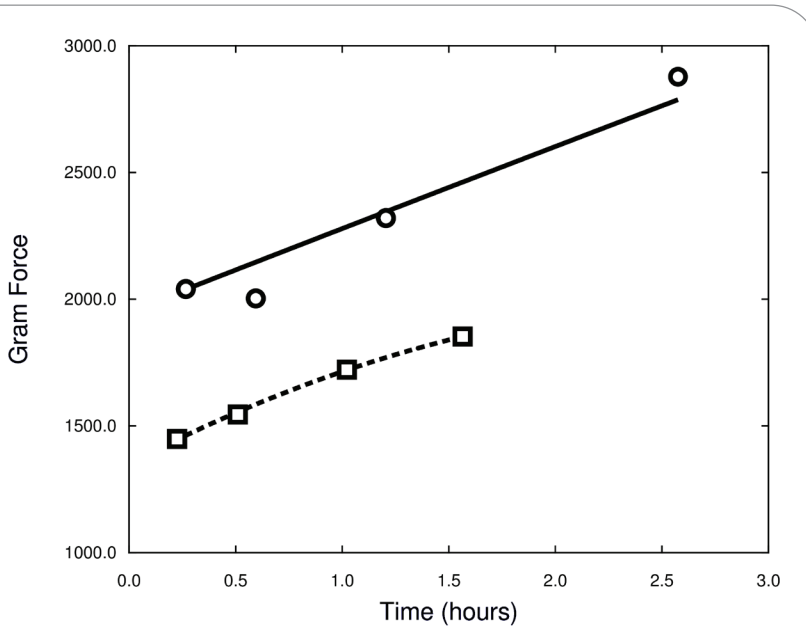


**FIGURE 16**

Comparison of scratch hardness development as a function of time for neat catalyzed topcoat vs. topcoat applied over 2 coats of stain and 1 coat of catalyzed sealer. Open circles and solid black line represent the neat topcoat; open square symbols and dashed line represent the finished system. Scratch hardness was obtained as load-to-stomata cracking.





The data of **Figure 17** were measured by the ADDTR in drying configuration and has been described previously.<sup>11</sup>

Tack-free time is given as the time required for the height of the drying trace

to reach 10% of the maximum peak height. Dry-hard time is the time for the height of the drying trace to reach the back side of the peak where the probe now rests approximately on the surface of the film.

The data show that tack-free time for UF1 and UF2 are similar, while dry-hard time for UF2 is faster by about 1 minute. UF3 displays faster tack-free and dry-hard times.

**FIGURE 17**  
ADDTR air-drying trace of three acid-curing varnishes, comparing three different UF resins.  
Test was conducted on films cast with 3 mil bird bar and 2-hour drying test.

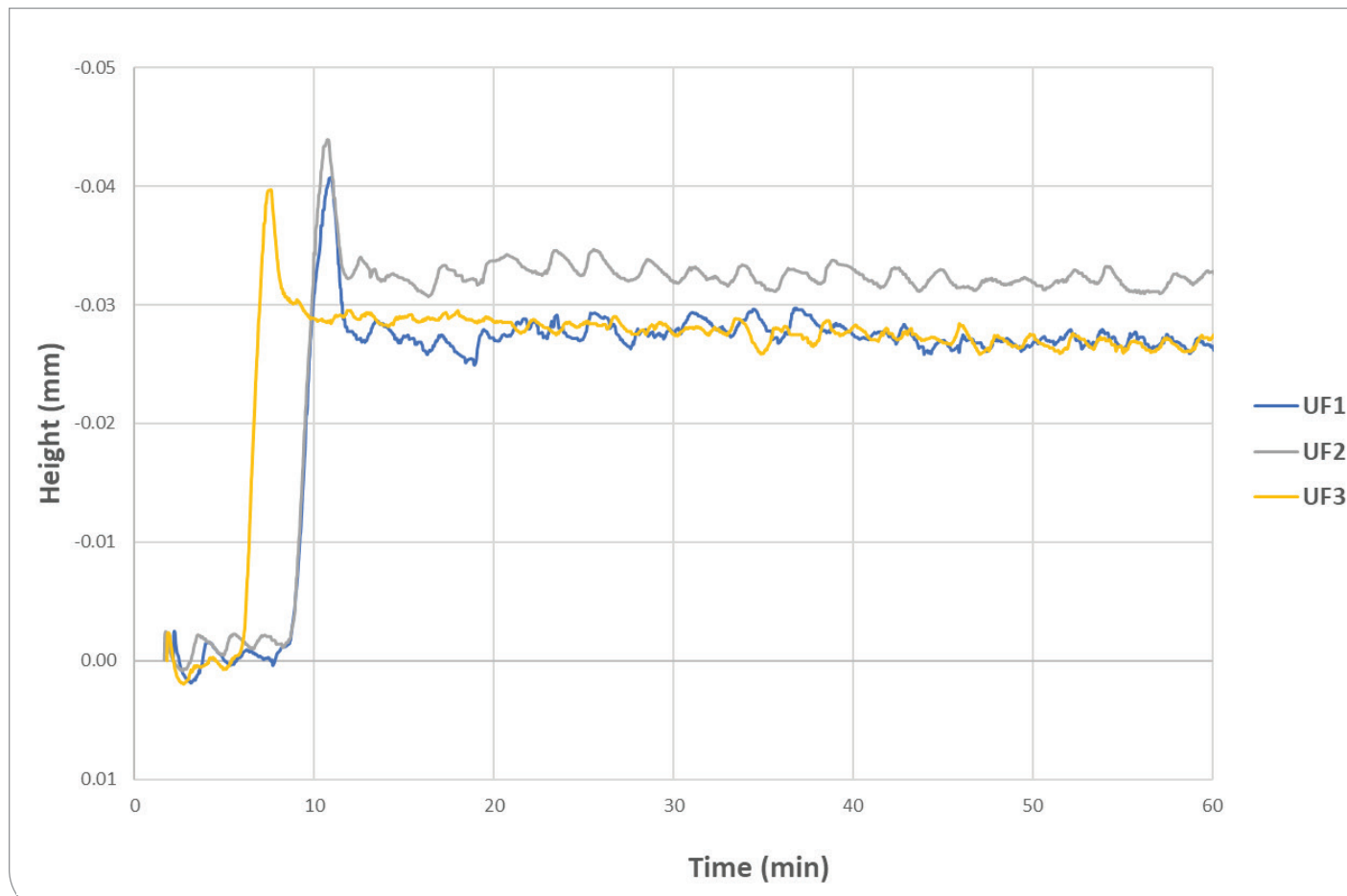


**Figure 18** displays viscosity versus cure time at 35 °C force-dry cure profile for the three varnishes displayed in **Figure 17**. While **Figure 19** compares force dry at 65 °C. The data indicate that force drying at 35 °C and 65 °C, as measured by viscosity, follows the same relative pattern as that for air drying displayed in **Figure 17**.

**Figure 20** displays storage modulus (green square symbols), loss modulus (green triangle symbols), and complex viscosity (green circle symbols) of the UF3 formulation as a function of cure time at 35 °C. The red square

and diamond indicate time of loss modulus/storage modulus crossover. Although the legend displays a calculated value of 184.48 seconds, the actual time from application is 362.46 seconds (6.04 minutes). The

6.04-minute timeframe is approximately equal to 6.17 minutes found for the tack-free time from the ADDTR drying trace.

**Table 5** summarizes tack-free and dry-hard times for samples as determined by

**TABLE 5**  
**Impact of UF Resin Composition on Air Drying of Acid-Cure Varnish**

UF Resin	ADDTR Tack-Free Time (min)	ADDTR Dry-Hard Time (min)	EDOT Sol-Gel Time (min)
UF1	8.88	12.82	8.17
UF2	8.92	11.88	6.73
UF3	6.17	10.07	6.04

**FIGURE 18**

The effect of UF resin chemistry on viscosity versus time at 35 °C for acid-catalyzed varnish. Gray symbols represent UF1; red symbols are UF2; and black symbols are UF3. 4.97% (w/w) catalyst.

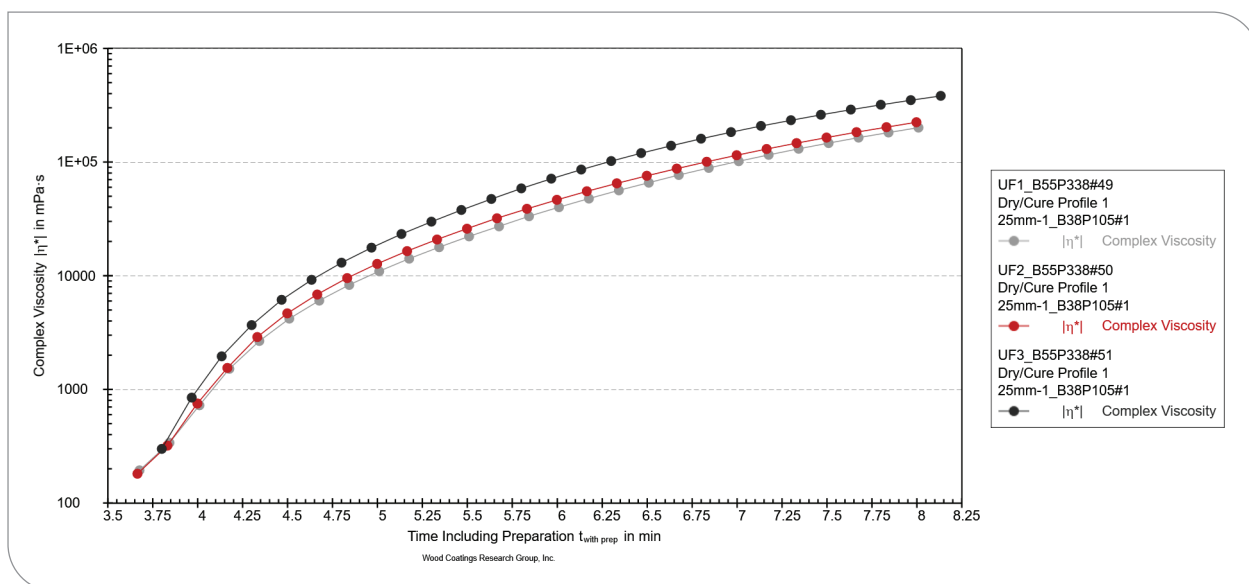
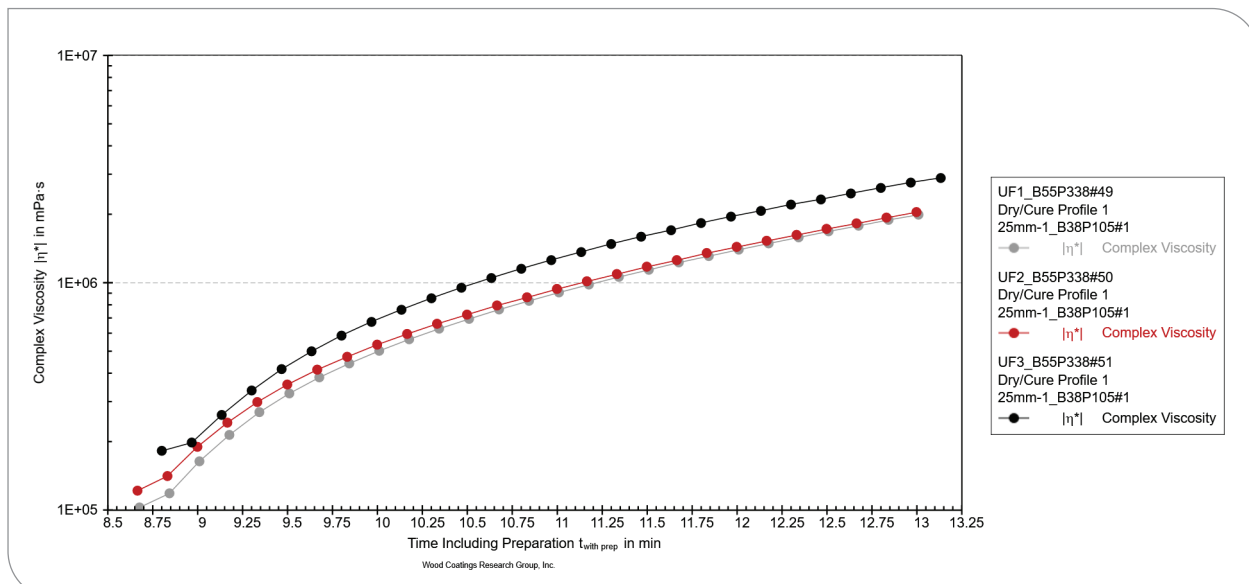


**FIGURE 19**

The effect of UF resin chemistry on viscosity vs. time at 65 °C for acid-catalyzed varnish. UF1 is represented by gray symbols; UF2 is represented by red symbols; UF3 is represented by black symbols; 4.97% (w/w) catalyst.



ADDTR, and storage modulus/loss modulus crossover times for samples measured by EDOT. The data of **Table 5** indicate that ADDTR tack-free time for these films applied by 3-mil bird bar corresponds approximately to sol-gel time as measured by EDOT with a 150-micron well plate. The discrepancy for UF2 may indicate that this sample responds to temperature faster than UF1.

Taking the data of the two methods together indicate that UF2 exhibits the characteristics of good lay-open time combined with fast “snap” cure. This is a desirable trait for wood finishes.

## Conclusions

Aminoplast-based coatings are a relatively mature technology, and much work has been accomplished in this arena. However, most kinetic work has focused on curing at high temperatures; further, the great quantity of quantitative data available appear to be based on film-hardness development after the sample has been cured under a cure protocol.

In this work, we have shown that cure of aminoplast coatings may be quantitatively assessed, from application to film consolidation, which allows the formulator and technologist to fill an important knowledge-base gap. Utilizing these methods, one may assess not only the impact of resin chemistry, but also solvent composition, catalyst chemistry, additives, pigments, etc., on cure.

In the current report, we have shown that rate of cure is dependent upon catalyst

concentration and temperature of cure. We found that for every 1 wt % catalyst solution addition, the time to reach sol-gel state of cure decreases linearly about 31.5 seconds between 1 wt % and 5.4 wt % catalyst addition, when evaluating over the entire cure protocol utilized. The rate of cure increases with catalyst concentration up to about 3% (w/w), and then levels off, (although slightly improving at 5.4% (w/w)) when force drying at 65 °C for short periods of time.

Scratch hardness is influenced by cure protocol, catalyst level, time of aging out of the oven, and the presence of preceding coating layers under the topcoat. Scratch hardness for a 5.4% catalyzed sample was found to increase rapidly after exposure to the cure protocol.

At low cure temperatures (35 °C), higher catalyst levels are required to increase rate of cure, curing rate increasing exponentially up to the maximum tested catalyst concentration of 5.4% (w/w), while at higher temperatures (65 °C) there appears to be a point reached where increasing catalyst concentration no longer yields significant cure-rate benefits. Solvent evaporation appears to play an important role in initial cure response, especially at 35 °C. Overall, we found that total rate of cure is dependent upon solvent evaporation (i.e., solvent composition), catalyst concentration and cure temperature.

Regarding  $T_g$  growth, 5.4 wt % catalyst addition was found to be about the optimum concentration for “off schedule” film

$T_g$  development in this specific formulation.  $T_g$  growth rate with catalyst concentration was found to fit a monomolecular growth model with a rate constant,  $k$ , of about 0.55.

Catalyst concentration was also found to impact the temperature at which the cross-linker responds. We found that catalyst levels as low as 1% results in a dramatic decrease in the temperature at which the crosslinker responds. Film glass-transition temperature was also found to increase as the catalyst concentration was increased. The data suggest that there is a maximum useful catalyst concentration.

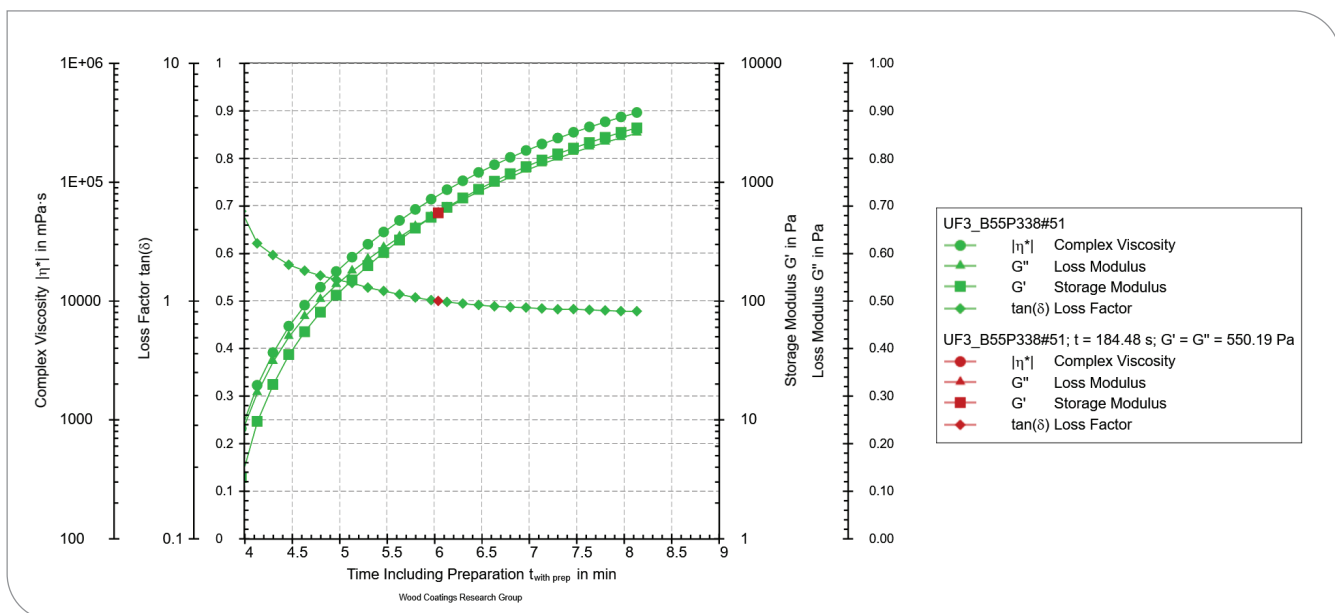
In comparing the influence of UF resin composition on drying rate, it was found that the methods discussed in this report can quantitatively distinguish cure rate between the three different UF resins evaluated. We found UF1 becomes tack-free approximately equal to UF2, while UF3 becomes tack-free significantly faster. On the other hand, dry-hard time and sol-gel time for the aminoplast resins increase in order UF1, requiring the longest time to dry, followed by UF2, and UF3 yielding the fastest drying time. We found that the higher molecular weight, partially isobutylated resin cures faster than a lower molecular weight resin. ♦

## References

1. Kirsch, A. *J. Amino Coating Resins, Their Invention and Reinvention*; Cytec Industries Inc., 1986, 1995; p 5. Library of Congress Catalog Card No. 86-72839.

continued on page 60

**FIGURE 20**  
Cure of UF3 crosslinker at 35 °C as measured by EDOT showing sol-gel, represented by the red square and red diamond symbols.



2. Wilson, R. C.; Pfohl, W. F. Study of Cross-Linking Reactions of Melamine/Formaldehyde Resin with Hydroxyl Functional Polyester by Generalized 2-D Infrared Spectroscopy. *Vibrat. Spectrosc.* **2000**, *23*, 13-22.
3. ASTM Standard D 1474-2013 R23, *Standard Test Methods for Indentation Hardness of Organic Coatings*; ASTM International: West Conshohocken, PA.
4. ASTM Standard E2546-15, *Standard Practice for Instrumented Indentation Testing*; ASTM International: West Conshohocken, PA.
5. ASTM Standard D 4366, *Standard Test Methods for Hardness of Organic Coatings by Pendulum Damping Tests*; ASTM International: West Conshohocken, PA.
6. ASTM Standard D 3363, *Standard Test Methods for Film Hardness of Organic Coatings by Pencil Test*; ASTM International: West Conshohocken, PA.
7. Blank, W. J. Reaction Mechanism of Amino Resin. *J. Coat. Technol.* **1979**, *51*, 61-70. [https://www.researchgate.net/publication/285529045REACTION\\_MECHANISM\\_OF\\_MELAMINE\\_RESINS](https://www.researchgate.net/publication/285529045REACTION_MECHANISM_OF_MELAMINE_RESINS).
8. Wood Coatings Research Group. Device for Measuring Drying, Curing, Film Formation, and Rheological Properties of Liquids and Films. U.S. Patent 10,451,533 B2, 2019.
9. Wood Coatings Research Group. Device for Measuring Drying, Curing, Film Formation, and Surface and Physical Properties of Liquids, Coatings, and Materials. U.S. Patent Application 63/152,973, 2021.
10. Obie, R. T. Evaporative Dynamic Oscillation (EDOT): A Versatile Technique for In Situ Characterization of Polymers and Coatings. *J. Coat. Technol. Res.* **2018**, *15*, 333-344.
11. Obie, R. T.; Anderson, C. A. Automated Dynamic Testing for Drying, Hardness, and Adhesion of Paints, Coatings and Adhesives. *Coatings Tech Mag.* **2022**, February, 40-56.
12. Swarthout, D.; Hogan, C. M. *Stomata. Encyclopedia of Earth*; National Council for Science and the Environment: Washington, DC, 2010.
13. Simfit - Simulation, Fitting, Statistics, and Plotting Software; Created by Bardsley, W. G.; University of Manchester, UK; Available at <https://simfit.org.uk>.
14. Tjørve, K. M. C.; Tjørve, E. The Use of Gompertz Models in Growth Analyses, and New Gompertz-Model Approach: An Addition to the Unified-Richards Family. *PLoS ONE* **2017**, *12* (6), e0178691. <https://doi.org/10.1371/journal.pone.0178691>.
15. Tjørve, E.; Tjørve, K. M. C. A Unified Approach to the Richards-Model Family for Use in Growth Analyses: Why We Need Only Two Model Forms. *J. Theor. Biol.* **2010**, *267*, 417-425. PMID: 20831877.

---

**Ronald Obie** is president at Wood Coatings Research Group, Inc. Email: [r.obie@woodcoatingsresearchgroup.com](mailto:r.obie@woodcoatingsresearchgroup.com)